Kinetics of Trypsin Inhibition by Its Specific Inhibitors

Jun-Mei Zhou, Chun Liu, and Chen-Lu Tsou*
Laboratory of Molecular Enzymology, Institute of Biophysics, Academia Sinica, Beijing, China
Received May 19, 1988; Revised Manuscript Received September 12, 1988

ABSTRACT: The kinetics of inhibition of trypsin by its specific inhibitors, pancreatic trypsin inhibitor, ovomucoid trypsin inhibitor, and soybean trypsin inhibitor, has been studied by following the hydrolysis of benzoylarginine ethyl ester in the presence of the inhibitor, and the results have been analyzed with the method described previously [Tian & Tsou (1982) *Biochemistry 21*, 1028]. The results obtained are consistent with the following: (a) The enzyme binds with the pancreatic inhibitor irreversibly to form an inactive complex. (b) The binding with the ovomucoid inhibitor to form the inactive complex is reversible. (c) An intermediate is formed before the relatively stable inactive complex with the soybean inhibitor, and both steps are reversible. The respective microscopic rate constants are determined by suitable plots of the apparent rate constants under different substrate and inhibitor concentrations. The second-order rate constants for the initial binding step thus obtained are in accord with the apparent inactivation rate constants determined by measuring the activity remaining with a stopped-flow apparatus equipped with a multimixing system after the enzyme–inhibitor mixture has been incubated for different time intervals.

Naturally occurring proteinase inhibitors are ubiquitous in animals, plants, and microorganisms, playing an important role in the regulation of many physiological processes. Trypsin inhibitors have been particularly extensively studied (Laskowski & Kato, 1980; Barrett & Salvesen, 1986) because of the general interest in specific protein–protein interaction, their physiological significance, and their possible medical implications. A large number of proteinacious trypsin inhibitors have been isolated and purified from different sources and their structures elucidated; these are classified usually according to their amino acid sequences and the structure of disulfide bridges they contain. Although the kinetics of the inhibition processes of these inhibitors have been investigated by a number of workers (Green, 1957; Putter, 1967; Haynes & Feeney, 1968), the conventional method of taking aliquots after the enzyme is mixed with the inhibitor and measuring the activity remaining was usually employed. In most cases, only the rate constant for the binding of the inhibitor with the enzyme could be obtained even when a stopped-flow apparatus was employed (Engel et al., 1974). As the activity measurements were usually made after dilution into the substrate-containing reaction mixture, dissociation of the reversibly formed enzyme–inhibitor complex to regenerate the free enzyme cannot be entirely avoided, especially in the presence of the substrate.

A kinetic method was proposed some years ago for the study of the rate of enzyme inhibition by following the substrate reaction in the presence of the inhibitor (Tsou, 1965a,b; Tian & Tsou, 1982; Wang & Tsou, 1987). Although irreversible inhibition kinetics has been mainly considered and subsequently applied to different systems in a number of laboratories (Harper & Powers, 1985; Mason et al., 1985; Tudela et al., 1986; Liu & Tsou, 1986; Ikam et al., 1987), the original treatment deals with both reversible and irreversible inhibitions. Similar treatments of the kinetics of substrate reaction in the presence of slow binding reversible inhibitors have also been dealt with by Levelliers et al. (1974), Cha (1975a,b, 1976), and Williams and Morrison (1979); however, the kinetic treatment of the progress of the substrate reaction in the presence of the inhibitor and data analysis are different from that proposed in the present series of studies. In this paper, analysis of the kinetic data of trypsin inhibition by its specific inhibitors with this method shows that PTI[1] inhibits apparently irreversibly, whereas inhibition by OTI and STI is reversible and an intermediate is discernible kinetically for STI. The determination of the respective microscopic rate constants is described.

Experimental Procedures

Materials. Trypsin, PTI, and STI were from Sigma, and OTI was from Rearal, Hungary. BAEE was from Dongfeng Biochemicals, Shanghai. All other reagents were local analytical grade reagents used without further purification.

Methods. Stock solutions of trypsin were made in 0.001 N HCl, and the concentration was determined by absorbance at 280 nm (Benmouyal & Trowbridge, 1966). The solution was stored at 4 °C and used within 3 days. Activity measurements were made at 25 °C with BAEE as substrate, and its hydrolysis was followed continuously by the increase in A_{253} with Cary 219 or Shimadzu UV 250 spectrophotometers thermostated at 25 °C. For kinetic studies, trypsin was added to a reaction mixture containing both the substrate and the inhibitor as specified in 50 mM Tris buffer, pH 7.8, containing 10 mM $CaCl_2$ to start the reaction. Unless otherwise specified, final concentrations of trypsin, BAEE, and the inhibitor were 0.06, 890, and 4.8 μM, respectively, in a total volume of 3 mL.

The apparent rate constants for the inhibition of trypsin by its specific inhibitors were also determined at 25 °C by the conventional method in a Durrum D-115K stopped-flow apparatus equipped with a Model D-132 multimixing system. Syringe A contained the enzyme and syringe B the inhibitor at an equal concentration. At zero time equal volumes of these were mixed, and after different times of incubation, usually from 20 ms to 5 s, these were again mixed with an equal volume of the reaction mixture in 50 mM Tris buffer, pH 7.8, containing 0.5 mM BAEE and 10 mM $CaCl_2$ in syringe C to start the reaction in a total volume of 0.6 mL. Final concentrations of the enzyme and the inhibitors were, for PTI,

* To whom correspondence should be addressed.

[1] Abbreviations: PTI, bovine pancreatic trypsin inhibitor; OTI, ovomucoid trypsin inhibitor; STI, soybean trypsin inhibitor; BAEE, benzoylarginine ethyl ester.

0006-2960/89/0428-1070$01.50/0

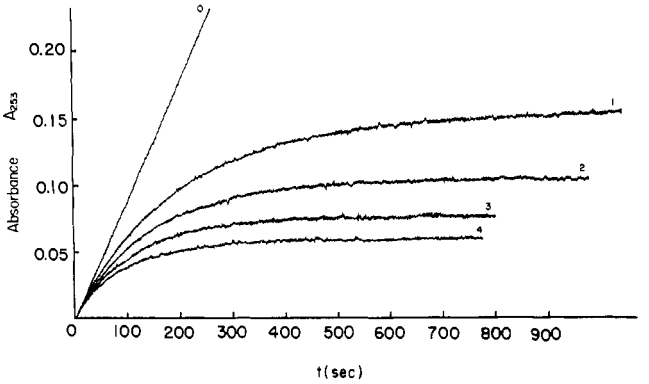

FIGURE 1: Hydrolysis of BAEE at different concentrations by trypsin in the presence of PTI. The enzyme concentration was 0.06 μM, and the concentration of PTI was 4.8 μM. Curve 0 is control without inhibitor, and curves 1–4 are progress curves with 890, 668, 445, and 223 μM of BAEE, respectively.

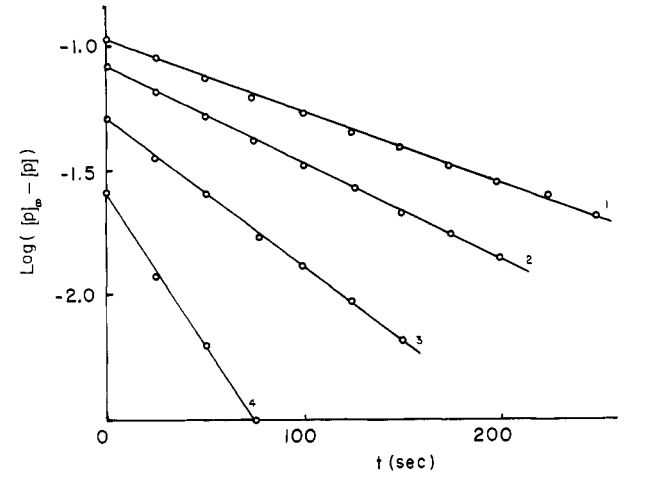

FIGURE 2: Semilogarithmic plots of log ($[P]_\infty$ – [P]) against t for the data given in Figure 1. The numbering of the lines is as for Figure 1.

0.75 μM, for OTI, 0.37 μM, and for STI, 0.57 μM. The initial straight-line portion was taken as a measure of the activity remaining at the time indicated.

RESULTS

Bovine Pancreatic Trypsin Inhibitor. Figure 1 shows the hydrolysis of BAEE at different concentrations in the presence of trypsin and PTI. It can be seen that with the lengthening of reaction time, the concentrations of product formed approach finite values, $[P]_\infty$, which decrease with decreasing concentrations of the substrate. This is as expected for competitive irreversible inhibitors from the relation $[P]_\infty = V[S]/k_3K_M[I]$ (Tsou, 1965a,b; Tian & Tsou, 1982), in which V is the maximal velocity without inhibitor, K_M is the Michaelis constant, k_3 is the rate constant for the binding of the inhibitor with the enzyme, and [S] and [I] are substrate and inhibitor concentrations, respectively. The apparent rate constant, A, can be obtained directly from the $[P]_\infty$ values by the relation $[P]_\infty = v/A[I]$, where v is the uninhibited reaction rate under otherwise identical conditions, or, alternatively, from the slopes of semilogarithmic plots (Figure 2) according to eq 1. A plot of $1/A$ against the substrate concentration, [S],

$$\log ([P]_\infty - [P]) = \log [P]_\infty - 0.434A[I] \quad (1)$$

shows that PTI is a competitive irreversible inhibitor as expected (Figure 3a), and as shown in eq 2, from the intercept

$$\frac{1}{A} = \frac{1}{k_3} + \frac{[S]}{k_3K_M} \quad (2)$$

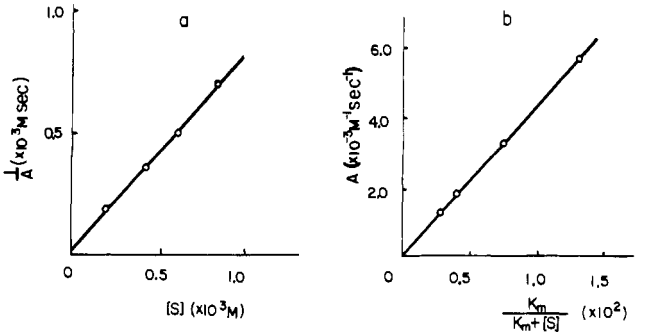

FIGURE 3: Determination of k_3 for the inhibition of trypsin by PTI from apparent rate constants measured at different [S] concentrations. Conditions were as for Figure 1. (a) Plot of $1/A$ against [S]; the y intercept gives $1/k_3$. (b) Plot of A against $K_M/(K_M)$ + [S)]; the slope gives k_3.

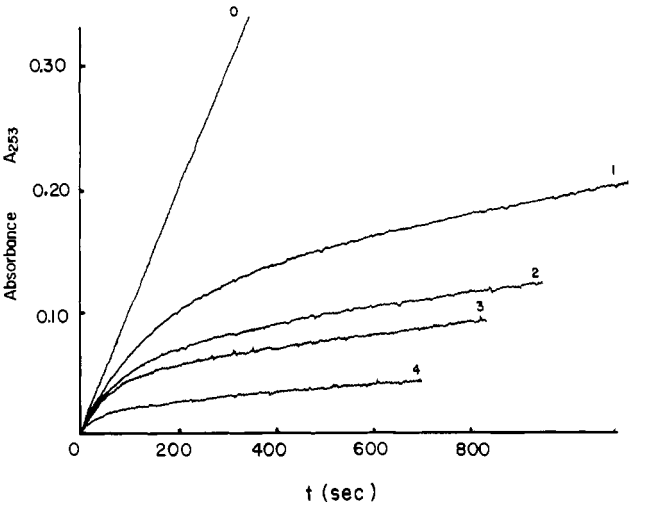

FIGURE 4: Hydrolysis of BAEE by trypsin in the presence of OTI. The control is indicated by 0, and concentrations of OTI for curves 1–4 were 0.87, 1.3, 1.73, and 3.46 μM, respectively.

on the y axis, the microscopic rate constant, k_3, for the reaction of the inhibitor with the enzyme can be obtained (Tian & Tsou, 1982). However, with high k_3 values as in the present case, the line intercepts the y axis at a point close to the origin, and consequently it is difficult to evaluate k_3 accurately. An alternative way to obtain k_3 is to plot A against $K_M/(K_M$ + [S]), and the slope gives directly the value of k_3 as shown in Figure 3b.

Ovomucoid Trypsin Inhibitor. Similar plots of the substrate reaction in the presence of OTI at different concentrations give a series of curves that, unlike the reactions in presence of PTI, do not approach finite values of $[P]_\infty$ with the lengthening of reaction time but a series of straight lines with positive slopes (Figure 4). Such a situation can arise either from a slow but reversible binding of the enzyme with the inhibitor or from some residual activity of the irreversibly formed EI complex. These two possibilities can be easily differentiated. If the enzyme–inhibitor association is reversible, the slopes of the straight lines should decrease with increasing inhibitor concentrations. On the other hand, if the EI complex is partly active, the slope of the straight lines should remain constant with higher inhibitor concentrations, but the approach to the straight line portions of the curves should become faster (Tsou, 1965b, 1988). An inspection of the curves in Figure 4 makes it clear that the former is the case, and the reaction between OTI and trypsin is reversible as indicated in

$$\begin{array}{ccccccc} S + E & \underset{k_{-1}}{\overset{k_1}{\rightleftharpoons}} & ES & \xrightarrow{k_2} & E + P & & (3) \\ + & & & & & & \\ I & & & & & & \\ {\scriptstyle k_3}\downarrow\uparrow{\scriptstyle k_{-3}} & & & & & & \\ EI & & & & & & \end{array}$$

The equation for product formation when the reaction between the inhibitor and the enzyme is reversible has been given before as (Tsou, 1965b; Tian & Tsou 1982)

$$[P] = v\left[\frac{B}{A[I] + B}t + \frac{A[I]}{(A[I] + B)^2}(1 - e^{-(A[I]+B)t})\right] \quad (4)$$

where v is the reaction rate in the absence of the inhibitor and B the apparent rate constant for the reverse reaction. When t is sufficiently large, the curves become straight lines with slopes $s = vB/(A[I] + B)$ and y-axis intercepts $i = vA[I]/(A[I] + B)^2$

$$[P] = \frac{vBt}{(A[I] + B)} + \frac{vA[I]}{(A[I]+ B)^2} \quad (5)$$

The apparent rate constants for the forward, A, and reverse, B, reactions can then be obtained.

Alternatively, subtracting eq 4 from eq 5 gives

$$[P]_{calc} - [P]_{obs} = v\frac{A[I]}{(A[I] + B)^2}e^{-(A[I]+B)t} \quad (6)$$

where $[P]_{calc}$ and $[P]_{obs}$ are the product concentrations as calculated from eq 5 and the value actually observed, respectively. A plot of log ($[P]_{calc} - [P]_{obs}$) against t should give a series of straight lines at different concentrations of the inhibitor with slopes of $-(A[I] + B)$. The apparent forward and reverse rate constants, A and B, can then be obtained. The value of B gives directly the microscopic rate constant, k_{-3}, and the value of k_3 can be obtained by suitable plots of A against [S] similarly as before either by a plot of $1/A$ against [S] or by a plot of A against $K_M/(K_M + [S])$ as shown in parts a and b of Figure 5. The results of the $1/A$ against [S] plot also show that, like PTI, OTI is a competitive inhibitor as expected. Furthermore, a plot of $1/A$ against [I] results in a straight line parallel with the x axis (Figure 5c), showing that no complex is formed prior to the inactivation step (Tian & Tsou, 1982).

Soybean Trypsin Inhibitor. The course of substrate reaction in the presence of STI as shown in Figure 6 is similar to those for OTI in that straight lines with positive slopes are approached without reaching finite values of $[P]_\infty$. However, a plot of log ($[P]_{calc} - [P]_{obs}$) against t in the case of STI gives a curve that can be resolved into two straight lines as shown in Figure 7, suggesting the formation of an intermediate for the binding of trypsin with this inhibitor. Included in the same figure for comparison is a similar plot for OTI that gives a single straight line. From the above, the mechanism of the inhibition of trypsin by STI appears to be a reversible and two-step process as given in

$$\begin{array}{ccccccc} S + E & \underset{k_{-1}}{\overset{k_1}{\rightleftharpoons}} & ES & \xrightarrow{k_2} & E + P & & (7) \\ + & & & & & & \\ I & & & & & & \\ {\scriptstyle k_3}\downarrow\uparrow{\scriptstyle k_{-3}} & & & & & & \\ EI & & & & & & \\ {\scriptstyle k_4}\downarrow\uparrow{\scriptstyle k_{-4}} & & & & & & \\ EI' & & & & & & \end{array}$$

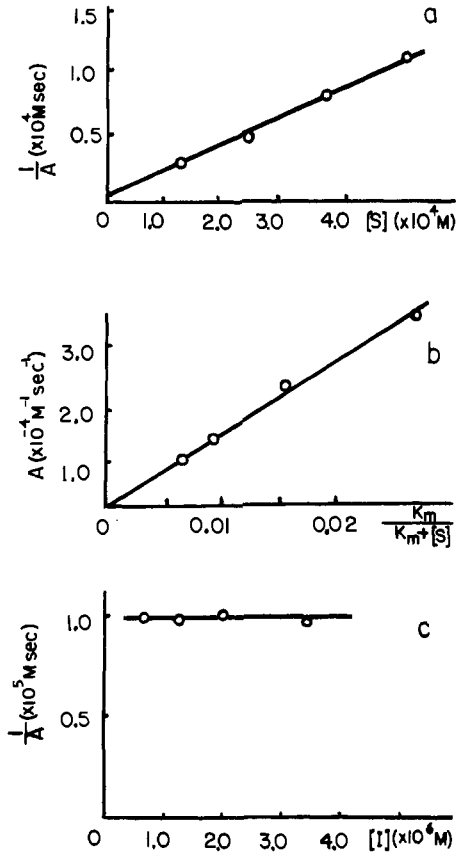

FIGURE 5: Plots to obtain the microscopic rate constants for the inhibition of trypsin by OTI. (a) Plot of $1/A$ against [S]. (b) Plot of A against $K_M/(K_M + [S])$. (c) Plot of $1/A$ against [I], showing noncomplexing inhibition.

It can be shown (see Appendix) that the formation of product [P] with time is

$$[P] = v_s t + P' - c_1 e^{-r_1 t} - c_2 e^{-r_2 t} \quad (8)$$

However, as shown in Figure 7 the plot of log ($[P]_{calc} - [P]_{obs}$) against time gives the curve resolvable into two straight lines with slopes of r_1 and r_2, which are

$$r_1 = \tfrac{1}{2}\left[k_{-3} + k_{-4} + k_4 + \frac{k_3K_m[I]}{k_m + [S]} + \left[\left(k_{-3} + k_{-4} + k_4 + \frac{k_3K_m[I]}{K_m + [S]}\right)^2 - 4\left(k_{-3}k_{-4} + (k_{-4} + k_4)\frac{k_3K_m[I]}{K_m + [S]}\right)\right]^{1/2}\right]$$

$$r_2 = \tfrac{1}{2}\left[k_{-3} + k_{-4} + k_4 + \frac{k_3K_m[I]}{K_m + [S]} - \left[\left(k_{-3} + k_{-4} + k_4 + \frac{k_3K_m[I]}{K_m + [S]}\right)^2 - 4\left(k_{-3}k_{-4} + (k_{-4} + k_4)\frac{k_3K_m[I]}{K_m + [S]}\right)\right]^{1/2}\right] \quad (9)$$

For each inhibitor concentration, a set of r_1 and r_2 values can be obtained, and it can be shown that

$$r_1 + r_2 = k_{-3} + k_4 + k_{-4} + \frac{k_3K_m}{K_m + [S]}[I]$$

$$r_1r_2 = k_{-3}k_{-4} + (k_{-4} + k_4)\frac{k_3K_m}{K_m + [S]}[I] \quad (10)$$

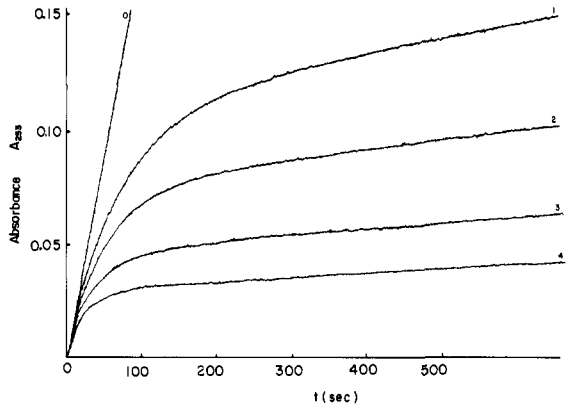

FIGURE 6: Hydrolysis of BAEE by trypsin in the presence of STI. The control is indicated by 0, and concentrations of STI for curves 1–4 were 0.75, 1.07, 1.71, and 2.68 μM, respectively. Enzyme concentration was 0.075 μM, and substrate concentration was 500 μM.

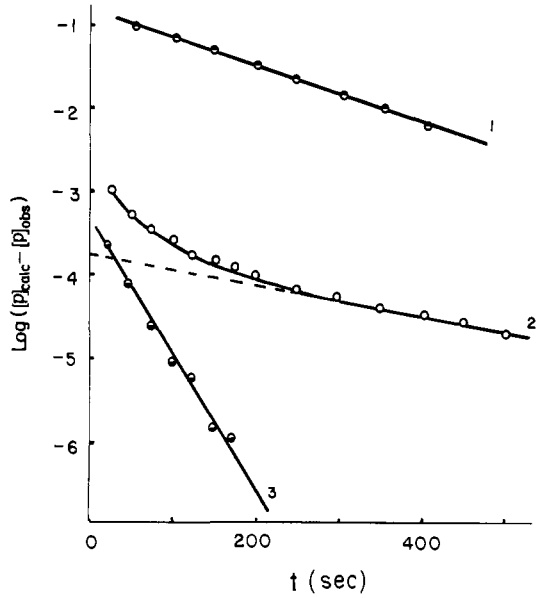

FIGURE 7: Plot of log ($[P]_{calc} - [P]_{obs}$) against t for the inhibition of trypsin by OTI and STI. Data are taken from curve 1 in Figure 4 for OTI (1) and from curve 3 in Figure 6 for STI (2). The deviation from the straight line in curve 2 gives the straight line 3 for the fast phase of inhibition by STI.

Table I: Microscopic Rate Constants of Trypsin Inhibition by Its Specific Inhibitors

	microscopic rate constants				10^6 app rate constant[a] (M^{-1} s^{-1})	
inhibitor	10^6k_3 (M^{-1} s^{-1})	10^6k_{-3} (M^{-1} s^{-1})	$10^{-3}k_4$ (s^{-1})	$10^{-3}k_{-4}$ (s^{-1})	this paper	lit.
PTI	0.37				0.59	0.28–1.1
OTI	1.5	0.4			1.3	2.2–3.4
STI	3.6	2.67	1.58	0.75	6.1	5.6–20

[a] The apparent inhibition rate constants were determined in the present investigation with a stopped-flow apparatus at pH 7.8, 25 °C. For sources of literature values, see text.

From the plots of $r_1 + r_2$ and r_1r_2 respectively against [I], the microscopic rate constants k_3, k_{-3}, k_4, and k_{-4} can be obtained. These plots are shown in Figure 8 and the rate constants summarized in Table I.

Constants Determined by the Conventional Method. For the study of the kinetics of the course of enzyme inhibition, the advantages of the present approach, following the course of reaction in the presence of both the enzyme and the inhibitor, over the conventional method, taking aliquots from

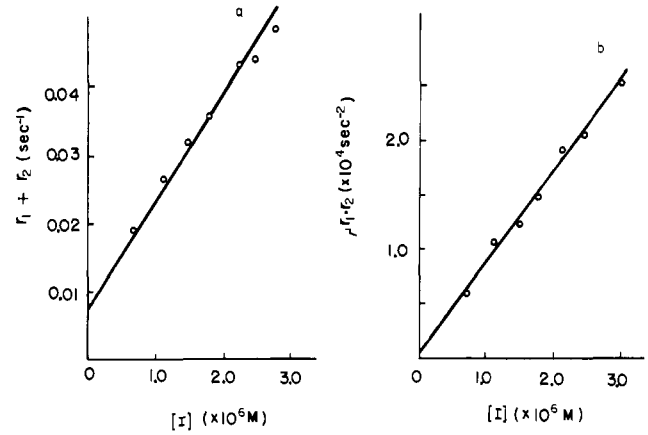

FIGURE 8: Plots to obtain the microscopic rate constant for the inhibition of trypsin by STI. The slopes, r_1 and r_2, are obtained for each STI concentration, and the values of (a) $r_1 + r_2$ and (b) r_1r_2 are plotted against [I] to give the rate constants k_3, k_{-3}, k_4, and k_{-4}. For details, see text.

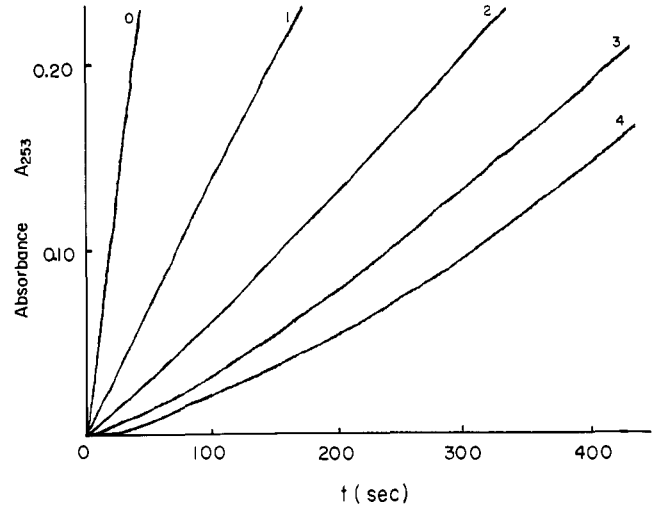

FIGURE 9: Course of hydrolysis of BAEE after different times of incubation of the enzyme with OTI. The reaction was started by adding 0.2 mL of the substrate to reaction mixtures containing 2.8 mL of both enzyme and OTI after times of incubation of 5, 20, 45, and 60 s for curves 1–4, respectively. Curve 0 represents the reaction in the absence of the inhibitor. Final concentrations of the substrate, enzyme, and OTI were 0.5 mM, 0.5 μM, and 0.5 μM, respectively.

an incubation mixture of the enzyme with the inhibitor at different time intervals for the measurement of remaining activity, have been discussed before (Tsou, 1965b, 1988; Tian & Tsou, 1982; Wang & Tsou, 1987). For slow binding reversible inhibitors, the conventional method has the added disadvantage that when the incubation mixture containing the enzyme and the inhibitor is diluted into the reaction mixture containing the substrate, the dissociation of the EI complex cannot be entirely avoided. The fractional activity remaining would depend on how fast the activity can be assayed after the dilution of the enzyme–inhibitor complex into the reaction mixture.

Figure 9 gives such an example in which after different times of incubation of OTI with the enzyme, the reaction was started by a small volume of the substrate to avoid unnecessary dilution. The hydrolysis of BAEE was then followed, and the gradual increase in the rates of hydrolysis is evident from the courses of reactions shown. The residue activity remaining depends very much on the time intervals taken for the measurement of the "initial" reaction rates. It is also evident from Figure 9 that for the particular case of inhibition of trypsin it is practically impossible to obtain the true initial rate and

consequently to determine the apparent rate constant accurately by manual operation. In the present investigation, measurements were made with a stopped-flow apparatus equipped with a multimixing system to obtain the true initial rates after the enzyme–inhibitor complex was diluted into the substrate-containing reaction mixture. The results thus obtained for the apparent inhibition rate constants for PTI, OTI, and STI are also listed in Table I. It can be seen that the apparent inhibition rate constants thus obtained by the conventional method are in satisfactory agreement with the microscopic rate constants, k_3, obtained for the association step of the enzyme with the inhibitors. Furthermore, these are also in accord with the values reported in the literature obtained by the conventional method (Green, 1957; Putter, 1967; Haynes & Feeney, 1968; Levilliers et al., 1974) or by directly measuring the enzyme–inhibitor binding rate with physicochemical methods with a stopped-flow apparatus (Luthy et al., 1971). The ranges of the values reported in the literature for these inhibitors are also included in Table I for comparison.

Discussion

For the interaction between trypsin and its inhibitor the following has been proposed as a standard overall mechanism (Findenstadt & Laskowski, 1965; Finkenstadt, 1974; Quast et al., 1978):

$$E + I = L = C = X = L^* = E + I^* \qquad (11)$$

L and L* are loose, noncovalent complexes that are rapidly dissociable, I* is the modified inhibitor, C is the stable enzyme–inhibitor complex, and X is the relatively stable intermediate before the chemical modification step. As the loose complexes L and L* are likely to be present in significant amount only at high inhibitor and enzyme concentrations and steps leading to the formation and subsequent reaction of these complexes are probably rapid reactions, the above can be simplified to (Laskowski et al., 1981)

$$E + I = C = X = E + I^* \qquad (12)$$

This is identical with the scheme presented above for STI. However, it should be pointed out that as inactivation rates were measured in the present study and C is the first relatively stable inactive complex, it is likely that the rate constants of the steps leading to the formation of C, E + I = L = C in eq 11 above, have been determined. The present investigation was carried out at pH 7.8, and it is unlikely that the step representing the hydrolysis of the susceptible bonds of the inhibitors, which has minimal rates at this pH for these inhibitors (Finkenstadt, 1974), can affect the results obtained.

Although the original kinetic treatment of the rate of enzyme inhibition was intended for both reversible and irreversible inhibitions [Tsou, 1965a,b; see Tian and Tsou (1982)], useful results have hitherto been obtained on irreversible inhibition kinetics only. This investigation shows that for the analysis of the kinetics of inhibitions by slow and reversible inhibitors the present approach of following the course of the substrate reaction in the presence of the inhibitor is equally applicable and has produced useful results. The kinetics of the tight binding trypsin inhibitors have been studied by earlier workers using usually the conventional method of following the course of inhibition by taking aliquots from the enzyme–inhibitor mixture at different time intervals and assaying for activity remaining (Green, 1957; Putter, 1967; Haynes & Feeney, 1968). Because of the inevitable dissociation of the enzyme–inhibitor complex upon dilution, especially in the presence of the substrate as shown in the present study, reliable results could only be obtained if care were taken to avoid unnecessary dilution and to take as far as possible the initial velocity for the measurements of the activity remaining. The latter, of course, can best be done with a stopped-flow apparatus (Engel et al., 1974).

Kinetic treatments of the substrate reaction during the action of slow and tight binding reversible inhibitors have been given by Levilliers et al. (1974), Cha (1975a,b, 1976), and Williams and Morisson (1979) as recently reviewed by Morrison and Walsh (1988). The tangents of the progress curve of the substrate reaction in the presence of the inhibitor were estimated by Cha (1976b) to obtain the rate of the substrate reaction at different time intervals of the reaction of the inhibitor with the enzyme for the determination of the rate constants. Although the equations describing the course of substrate reaction in the presence of the inhibitor given by Levilliers et al. [eq 6 in Levilliers et al. (1974)] and by Williams and Morrison (1988) are similar to an equation originally presented by one of us [Tsou, 1965b, eq 8; see also Tian and Tsou (1982)], the methods of analysis of the results are entirely different. As shown in the present investigation, the approach of following the progress curve of the substrate reaction in the presence of the inhibitor has the advantages of not only being able to deal with reactions too fast to be conveniently followed by taking aliquots from the reaction mixture at different time intervals but also in providing useful information in the mechanism of action of the inhibitors and in the determination of the microscopic rate constants.

Among the inhibitors studied, it is interesting to note that only PTI follows apparently irreversible kinetics as [P] approaches a constant value with increasing reaction time. As finite time intervals only can be followed experimentally, the above results do not exclude the possibility of reversible enzyme inhibitor binding with a dissociation rate too slow to be detected during the time interval under observation. In this connection, it is interesting to note that the dissociation rate constant was reported to be 6.6×10^{-8} s^{-1} by Vincent and Lazdunski (1972) for the complex of trypsin with this inhibitor. In fact, it is so stable that the dissociation is a slow process even in 8 M urea or 6 M guanidine (Levilliers et al., 1970). The difference between PTI and OTI on the one hand and STI on the other may also be explained by a large difference in the magnitude of the respective rate constants for PTI and OTI, so that only one of these can be obtained. The three inhibitors studied in the present paper belong to different families classified according to their amino acid sequences and the structures of their disulfide bonds (Laskowski & Kato, 1980). The fact that they behave differently may not be entirely accidental. Whether the difference in kinetic behavior is in any way related to the difference in their chemical structures among members of different families of trypsin inhibitors will be well worth looking into.

Appendix

The scheme for substrate hydrolysis catalyzed by trypsin in the presence of STI can be written

$$\begin{array}{ccccc} S + E & \underset{k_{-1}}{\overset{k_1}{\rightleftharpoons}} & ES & \xrightarrow{k_2} & E + P \\ + & & & & \\ I & & & & \\ k_3 \downarrow \uparrow k_{-3} & & & & \\ EI & & & & \\ k_4 \downarrow \uparrow k_{-4} & & & & \\ EI' & & & & \end{array} \qquad (A1)$$

Let

$$[E_T] = [E] + [ES] \quad (A2)$$

$$[E]_0 = [E_T] + [EI] + [EI'] \quad (A3)$$

The rate of formation of [EI'] can be written

$$\frac{d[EI']}{dt} = -\frac{d[E_T]}{dt} - \frac{d[EI]}{dt} = k_{+4}[EI] - k_{-4}([E]_0 - [E_T] - [EI]) \quad (A4)$$

From the relation $d[E_T]/dt = k_{-3}[EI] - k_3[E][I]$, it can be shown that

$$\frac{d^2[E_T]}{dt^2} + \left(k_{-3} + k_{-4} + k_4 + \frac{k_3K_m}{K_m + [S]}[I]\right)\frac{d[E_T]}{dt} + \left[k_{-3}k_{-4} + k_3(k_{-4} + k_4)\frac{K_m[I]}{K_m + [S]}\right][E_T] - k_{-3}k_{-4}[E]_0 = 0 \quad (A5)$$

and

$$[E_T] = a_1e^{-r_1t} + a_2e^{-r_2t} + \frac{k_{-3}k_{-4}[E_0]}{k_{-3}k_{-4} + k_3(k_{-4} + k_4)\frac{K_m}{K_m + [S]}[I]} \quad (A6)$$

where a_1 and a_2 are constants and r_1 and r_2 are given by

$$r_1 = \tfrac{1}{2}\left[k_{-3} + k_{-4} + k_4 + \frac{k_3K_m[I]}{k_m + [S]} + \left[\left(k_{-3} + k_{-4} + k_4 + \frac{k_3K_m[I]}{K_m + [S]}\right)^2 - 4\left(k_{-3}k_{-4} + (k_{-4} + k_4)\frac{k_3K_m[I]}{K_m + [S]}\right)\right]^{1/2}\right]$$

$$r_2 = \tfrac{1}{2}\left[k_{-3} + k_{-4} + k_4 + \frac{k_3K_m[I]}{K_m + [S]} - \left[\left(k_{-3} + k_{-4} + k_4 + \frac{k_3K_m[I]}{K_m + [S]}\right)^2 - 4\left(k_{-3}k_{-4} + (k_{-4} + k_4)\frac{k_3K_m[I]}{K_m + [S]}\right)\right]^{1/2}\right] \quad (A7)$$

The formation of the product at time t is then

$$[P] = \frac{k_{-3}k_{-4}vt}{k_{-3}k_{-4} + k_3(k_{-4} + k_4)\frac{K_m[I]}{K_m + [S]}} + P' - c_1e^{-r_1t} - c_2e^{-r_2t} \quad (A8)$$

where v is the reaction rate in the absence of the inhibitor and P' is given by

$$P' = C_1 + C_2 = \frac{v\frac{k_3K_m[I]}{k_m + [S]} - (v - v_S)r_2}{(r_1 - r_2)r_1} + \frac{v\frac{k_3K_m[I]}{K_m + [S]} - (v - v_s)r_1}{(r_2 - r_1)r_2} \quad (A9)$$

As t approaches infinity, the above becomes a straight line

$$[P] = v_st + P' \quad (A10)$$

and subtracting eq A8 from eq A10 gives

$$[P]_{calc} - [P]_{obs} = C_1e^{-r_1t} + C_2e^{-r_2t} \quad (A11)$$

It can be seen from eq All that in a plot of log $([P]_{calc} - [P]_{obs})$ against t, as given in Figure 7, the curve obtained can be resolved into two straight lines with slopes of r_1 and r_2, respectively, and $r_1 + r_2$ and r_1r_2 are

$$r_1 + r_2 = k_{-3} + k_4 + k_{-4} + \frac{k_3K_m}{K_m + [S]}[I]$$

$$r_1r_2 = k_{-3}k_{-4} + (k_{-4} + k_4)\frac{k_3K_m}{K_m + [S]}[I] \quad (A12)$$

The microscopic constants k_3, k_{-3}, k_4, and k_{-4} can then be calculated from the slopes and the intersects of the straight lines obtained by plotting $r_1 + r_2$ and r_1r_2, respectively, against [I].

Registry No. STI, 9078-38-0; PTI, 9087-70-1; trypsin, 9002-07-7.

References

Barrett, A. J., & Salvesen, G. (1986) in *Proteinase Inhibitors*, pp 301–627, Elsevier, Amsterdam.

Benmouyal, P., & Trowbridge, C. G. (1966) *Arch. Biochem. Biophys. 115*, 67–76.

Cha, S. (1975a) *Biochem. Pharmacol. 24*, 2177–2185.

Cha, S. (1975b) *Biochem. Pharmacol. 24*, 2187–2197.

Cha, S. (1976) *Biochem. Pharmacol. 25*, 2695–2702.

Engel, J., Quast, U., Heumann, H. Krause, G., & Steffin, E. (1974) in *Proteinase Inhibitors* (Fritz, H., Tshesche, H., Greene, L. J., & Truscheit, E., Eds.) pp 412–419, Springer-Verlag, Berlin.

Findenstadt, W. R., & Laskowski, M., Jr. (1965) *J. Biol. Chem. 240*, PC962–963.

Finkenstadt, W. R., Hamid, M. A., Mattis, J. A., Schrode, J., Sealock, R. W., Wang, D., & Laskowski, M., Jr. (1974) in *Proteinase Inhibitors* (Fritz, H., Tshesche, H., Greene, L. J., & Truscheit, E., Eds.) pp 389–411, Springer-Verlag, Berlin.

Green, N. M. (1957) *Biochem. J. 66*, 407–415.

Harper, J. W., & Powers, J. C. (1985) *Biochemistry 24*, 7200–7213.

Haynes, R., & Feeney, R. E. (1968) *Biochemistry 7*, 2879–2885.

Ikam, C.-M., Copher, J. C., & Powers, J. C. (1987) *J. Am. Chem. Soc. 109*, 5044–5045.

Laskowski, M., Jr., & Kato, I. (1980) *Annu. Rev. Biochem. 49*, 593–626.

Laskowski, M., Jr., Empie, M. W., Kato, I., Kohr, W. J., Ardelt, W., Bogard, W. C., Jr., Weber, E., Papamokos, E., Bode, W., & Huber, R. (1981) in *Structural and Functional Aspects of Enzyme Catalysis* (Eggerer, R., & Huber, R., Eds.) pp 136–152, Springer-Verlag, Heidelberg.

Levilliers, N., Peron-Renner, M., Arrio, B., & Pudles, J. (1970) *Arch. Biochem. Biophys. 140*, 474–483.

Levilliers, N., Peron-Renner, M., & Pudles, J. (1974) in *Proteinase Inhibitors* (Fritz, H., Tshesche, H., Greene, L. J., & Truscheit, E., Eds.) pp 432–444, Springer-Verlag, Berlin.

Liu, W., & Tsou, C. L. (1986) *Biochim. Biophys. Acta 870*, 185–190.

Luthy, J. A., Praissman, M., Finkenstadt, W. R., & Laskowski, M., Jr. (1971) *J. Biol. Chem. 248*, 1760–1771.

Mason, R. W., Green, G. D. J., & Barrett, A. J. (1985) *Biochem. J. 226*, 233–141.

Morrison, J. F., & Walsh, C. T. (1988) *Adv. Enzymol. Relat. Areas Mol. Biol. 61*, 201–301.

Putter, J. (1967) *Z. Physiol. Chem. 348*, 1197–1206.

Quast, U., Engel, J., Steffen, E., Tschsche, H., & Kupfer, S. (1978) *Eur. J. Biochem. 86*, 353–360.

Tian, W. X., & Tsou, C. L. (1982) *Biochemistry 21*, 1028–1032.

Tsou, C. L. (1965a) *Acta Biochim. Biophys. Sin. 5*, 398-408.
Tsou, C. L. (1965b) *Acta Biochim. Biophys. Sin. 5*, 409-417.
Tsou, C. L. (1988) *Adv. Enzymol. Relat. Areas Mol. Biol. 61*, 381-436.
Tudela, J., Garcia-Canovas, F., Garcia-Carmona, F., Iborra, J. L., & Lozano, J. A. (1986) *Int. J. Biochem. 18*, 285-288.
Vincent, J. P., & Lazdunski, M. (1972) *Biochemistry 11*, 2967-2977.
Wang, Z. X., & Tsou, C. L. (1987) *J. Theor. Biol. 127*, 253-270.
Williams, J. W., & Morrison, J. F. (1979) *Methods Enzymol. 63*, 437-467.

Linking Number Anomalies in DNA under Conditions Close to Condensation†

Steven Ringquist,‡ Rina Shinn, and Sue Hanlon*
Department of Biological Chemistry, University of Illinois College of Medicine, Chicago, Illinois 60612
Received June 20, 1988; Revised Manuscript Received September 16, 1988

ABSTRACT: Changes in linking number and the apparent winding angle of pBR322 DNA have been evaluated in mixed ethanol–water solvents containing either Na or Mg as the major counterion contributing to the electrostatic shielding of the duplex. The average number of superhelical turns (τ) produced in the standard electrophoresis buffer (Tris–borate–EDTA, pH 8.0) by the transfer of DNA, relaxed in 200 mM NaCl, 10 mM NaH_2PO_4/Na_2HPO_4, and 2 mM EDTA, pH 7, by calf thymus topoisomerase or ligated in 6.6 mM $MgCl_2$, 1 mM KCl, 1 mM ATP, 1 mM dithiothreitol, and 66 mM Tris, pH 7.6, by T4 ligase, was determined as a function of the EtOH concentration. At low enzyme concentrations, the τ values became increasingly more positive in the presence of both cations as the ethanol concentration increased, indicating that the duplex structure was overwound in the ethanol solvents. Winding angle changes between 0 and 20% ethanol, calculated from these values of τ, exhibited the same correlations with CD spectral properties as had been previously observed for 100% aqueous systems containing monovalent cations [Kilkuskie, R., Wood, N., Shinn, R., Ringquist, S., & Hanlon, S. (1988) *Biochemistry 27*, 4377-4386]. The results at higher concentrations of ethanol (25–30%), however, were anomalous for the Mg–ligase system. The anomalies increased with higher ethanol, ligase, or Mg concentration. Gel run under these conditions showed enhanced concentrations of slow-moving components, indicative of ligation of intermolecular associated DNA species. At a 10-fold higher level of ligase, ethanol appeared to unwind the duplex, confirming the results of Lee, Mizusawa, and Kakefuda [(1981) *Proc. Natl. Acad. Sci. U.S.A. 78*, 2838-2842]. All of these anomalies occur under solvent conditions which are close to conditions which produce a heterogeneous dispersion of sedimenting species in ultracentrifugal experiments and compact rodlike structures, visualized by electron microscopy. The circular dichroism spectra at the onset of the formation of these structures show the characteristics of a chirally packed array of DNA duplexes. The reversal of the trend of the ethanol effect on linking number at higher enzyme and Mg(II) concentrations can be most easily explained by the promotion of the condensation phenomenon by either the ligase or a contaminating factor in the preparation. We suggest that the anomalies in the linking number and winding angle values are due to either ligation of chirally bent DNA species or a change in the helical period as the linear DNA adapts to the conformation required for collapse. At ethanol concentrations well below that required for DNA collapse, the average change in winding angle calculated from the relative linking number appears to be valid and independent of whether the relaxed DNA species was produced by the topoisomerase or the ligase. In the absence of condensation effects, CD changes are also a reliable index of small *average* winding angle changes in random-sequence B-form DNA in ethanol. Winding angle changes cannot, however, be reliably evaluated by gel methods at or close to conditions where chiral collapse or condensation of DNA occurs.

A number of observations conducted with random-sequence DNA have confirmed the correlation between winding angle changes and the circular dichroism (CD)[1] spectral properties. As long as an average B backbone geometry is mainained, an increase in the average winding angle of DNA in aqueous solutions is accompanied by a decrease in the rotational strength of the positive band above 260 nm in the CD spectrum (Johnson et al., 1981; Baase & Johnson, 1979; Chan et al., 1979; Kilkuskie et al., 1988). The conditions which produce changes in winding angle almost certainly produce other structural changes and have extraneous ion and solvent effects, but these seem to be coordinated with the winding angle changes. Thus, winding angle changes produced by the covalent attachment of a charged amine in the groove of the duplex have the same effect on rotational strength as do changes in the electrolyte content of the aqueous solvent environment (Kilkuskie et al., 1988).

Prior to undergoing the B → A transition in mixed aqueous–alcohol solvents, the CD spectra of a variety of DNAs

† Taken in part from the Ph.D. Thesis of S.R. This work was supported by a grant from the National Institutes of Health (GM 30284).
* To whom correspondence should be addressed.
‡ Present address: Department of Genetics & Development, College of Physicians and Surgeons, Columbia University, New York, NY.

[1] Abbreviations: EDTA, sodium ethylenediaminetetraacetate; EtOH, ethanol; CD, circular dichroism; bp, base pair(s); Lk, linking number; Wr, writhe; Tw, twist; DTT, dithiothreitol; SDS, sodium dodecyl sulfate.

0006-2960/89/0428-1076$01.50/0